

(19) World Intellectual Property Organization
International Bureau



(43) International Publication Date
15 November 2001 (15.11.2001)

PCT

(10) International Publication Number
WO 01/86038 A2

(51) International Patent Classification⁷: **C30B 29/60**

(21) International Application Number: PCT/CA01/00621

(22) International Filing Date: 4 May 2001 (04.05.2001)

(25) Filing Language: English

(26) Publication Language: English

(30) Priority Data:
60/202,115 5 May 2000 (05.05.2000) US

(71) Applicants (*for all designated States except US*): **UNIVERSIDAD POLITECNICA DE VALENCIA** [ES/ES]; Camino de Vera, 14, E-46022 Valencia (ES). **CONSEJO SUPERIOR DE INVESTIGACIONES CIENTIFICAS** [ES/ES]; Serrano, 117, E-28006 Madrid (ES).

(71) Applicants and

(72) Inventors: **MIGUEZ GARCIA, Hernan** [ES/CA]; c/o University Of Toronto, Department of Chemistry, Lash Miller Chemical Laboratories, 80 St. George

Street, Toronto, Ontario M5S 3H6 (CA). **JOHN, Sajeev** [CA/CA]; 1087 Staghorn Court, Mississauga, Ontario L5C 3R2 (CA). **CHOMSKI, Emmanuel, Benjamin** [CA/CA]; 30 McEwen Avenue, Apt #704, Ottawa, Ontario K2B 5K8 (CA).

(72) Inventors; and

(75) Inventors/Applicants (*for US only*): **LOPEZ FERNANDEZ, Ceferino** [ES/ES]; Avenida de Castilla la Mancha 33, B-1, San Sebastian de los Reyes, E-28700 Madrid (ES). **MESEGUER RICO, Francisco, Javier** [ES/ES]; Avenida del Saler, 8, flat 26th, E-46013 Valencia (ES). **OZIN, Geoffrey, Alan** [CA/CA]; 63 Gormley Avenue, Toronto, Ontario M4V 1Y9 (CA).

(74) Agent: **HILL & SCHUMACHER**; Suite 802, 335 Bay Street, Toronto, Ontario M5H 2R3 (CA).

(81) Designated States (*national*): AE, AG, AL, AM, AT, AU, AZ, BA, BB, BG, BR, BY, BZ, CA, CH, CN, CO, CR, CU, CZ, DE, DK, DM, DZ, EE, ES, FI, GB, GD, GE, GH, GM, HR, HU, ID, IL, IN, IS, JP, KE, KG, KP, KR, KZ, LC, LK, LR, LS, LT, LU, LV, MA, MD, MG, MK, MN, MW, MX,

[Continued on next page]

(54) Title: **PHOTONIC BANDGAP MATERIALS BASED ON GERMANIUM**



(57) **Abstract:** Photonic bandgap materials based on germanium and methods of synthesis of germanium based photonic band gap (PBG) materials. The synthesis and characterization of high quality, very large scale, face centered cubic photonic band gap (PBG) materials consisting of pure germanium, exhibiting three-dimensional PBGs in the near infrared region. This is obtained by two different methods: (1) infiltrating a self-assembling silica opal template with a germanium alkoxide which is later hydrolyzed to form germanium(IV) oxide. This compound is then reduced to germanium(0) in a hydrogen atmosphere. This cycle is repeated until the desired germanium infiltration is attained. Once the germanium guest lattice is formed, the template is removed and a germanium inverse opal is obtained. (2) Chemical vapor deposition of germanium into a self-assembling silica opal template, and subsequent removal of the template. This achievement realizes a long standing goal in photonic materials and opens a new door for complete control of radiative emission from atoms and molecules, light localization and the integration of micron scale photonic devices into a three-dimensional all-optical micro-chip.

BEST AVAILABLE COPY

WO 01/86038 A2



MZ, NO, NZ, PL, PT, RO, RU, SD, SE, SG, SI, SK, SL,
TJ, TM, TR, TT, TZ, UA, UG, US, UZ, VN, YU, ZA, ZW.

(84) Designated States (regional): ARIPO patent (GH, GM, KE, LS, MW, MZ, SD, SL, SZ, TZ, UG, ZW), Eurasian patent (AM, AZ, BY, KG, KZ, MD, RU, TJ, TM), European patent (AT, BE, CH, CY, DE, DK, ES, FI, FR, GB, GR, IE, IT, LU, MC, NL, PT, SE, TR), OAPI patent (BF, BJ, CF, CG, CI, CM, GA, GN, GW, ML, MR, NE, SN, TD, TG).

Published:

— without international search report and to be republished upon receipt of that report

For two-letter codes and other abbreviations, refer to the "Guidance Notes on Codes and Abbreviations" appearing at the beginning of each regular issue of the PCT Gazette.

PHOTONIC BANDGAP MATERIALS BASED ON GERMANIUM

FIELD OF THE INVENTION

5 The present invention relates to a method of synthesis of periodic composite materials of germanium and another material with a dielectric constant less than germanium, and more particularly the invention relates to photonic band gap (PBG) materials based on germanium having complete photonic bandgaps.

10 BACKGROUND OF THE INVENTION

Photonics is the science of molding the flow of light. Photonic band gap (PBG) materials, as disclosed in S. John, Phys. Rev. Lett. 58, 2486 (1987), and E. Yablonovitch, Phys. Rev. Lett. 58, 2059 (1987), are a new class of dielectrics which carry the concept of molding the flow of light to its ultimate level, namely by facilitating the coherent localization of light, see S. John, **Phys. Rev. Lett.** 53, 2169 (1984), P. W. Anderson, **Phil. Mag. B** 52, 505 (1985), S. John, **Physics Today** 44, no. 5, 32 (1991), and D. Wiersma, D. Bartolini, A. Lagendijk and R. Righini, **Nature** 390, 671 (1997). This provides a mechanism for the control and inhibition of spontaneous emission of light from atoms and molecules forming the active region of the PBG materials, and offers a basis for low threshold micro-lasers and novel nonlinear optical phenomena. Light localization within a PBG facilitates the realization of high quality factor micro-cavity devices and the integration of such devices through a network of microscopic wave-guide channels (see J. D. Joannopoulos, P.R. Villeneuve and S. Fan, **Nature** 386, 143 (1998)) within a single all-optical microchip. Since light is caged within the dielectric microstructure, it cannot scatter into unwanted modes of free propagation and is forced to flow along engineered defect channels between the desired circuit elements. PBG materials, infiltrated with suitable liquid crystals, may exhibit fully tunable photonic band structures [see K. Busch and S. John,

15
20
25

Phys. Rev. Lett. 83, 967 (1999) and E. Yablonovitch, **Nature** 401, 539 (1999)] enabling the steering of light flow by an external voltage. These possibilities suggest that PBG materials may play a role in photonics, analogous to the role of semiconductors in conventional microelectronics. As pointed out by Sir John Maddox, "If only it were possible to make dielectric materials in which electromagnetic waves cannot propagate at certain frequencies, all kinds of almost magical things would be possible." John Maddox, **Nature** 348, 481 (1990).

The single biggest obstacle to the realization of these photonic capabilities is the lack of a proven route for synthesis of high quality, very large-scale PBG materials with significant electromagnetic gaps at micron and sub-micron wavelengths. The method of micro-fabrication must also allow the controlled incorporation of line and point defects, for optical circuitry, during the synthetic process.

One very promising material for use in producing photonic devices is germanium. Producing photonic devices from germanium-based photonic crystals would be a very significant commercial advantage since methods of fabricating such materials could be readily retrofitted into existing germanium chip fabrication facilities.

Nature produces optically unique materials based on silica. Specifically, opals are semiprecious stones used in jewelry and decoration. The structure of naturally occurring opals was discovered for the first time in 1964 [J.V. Sanders, **Nature** 1964]. They are macroporous materials made by a periodic distribution of silica sub-micrometer spheres embedded in a silica medium with a slightly different refractive index. They present iridescent colors due to Bragg diffraction of light as a consequence of the three dimensional periodic modulation of the dielectric contrast in the structure. Owing to their potential technologic applications, the fabrication of artificial opals has become a significant goal in the field of optics.

It is very advantageous to use artificial opals as a template from which to produce inverse opals comprising germanium. In this way the periodicity of the self-assembling opal template is transferred to the inverse opal. A large scale periodic microstructure is thereby produced efficiently and at low cost, without recourse to time consuming and expensive photolithography (see S. John and K. Busch, **Journal of Lightwave Technology IEEE**, volume 17, number 11, pages 1931-1943, (1999)). Up to this point in time, conventional photolithography has produced only very small scale structures, with a very small number of repeating unit cells (see S.Y. Lin and J.G. Fleming, **J. of Lightwave Technology IEEE**, 17, no.11, 1944 (1999) and S. Noda et al. *ibid*, 1948 (1999)). This method is effective for creating two-dimensional patterns, but does not readily lend itself to the production of large-scale three-dimensional periodic structures.

It is particularly advantageous to provide a method which can produce inverse germanium opals with lattice constants spanning the range from which useful photonic devices could be produced and which at the same time is scalable to a very large number of repeating unit cells. With such a germanium inverse opal, a large number of photonic devices can be integrated into a single three-dimensional optical chip.

SUMMARY OF THE INVENTION

It is an object of the present invention to provide a method for synthesizing periodic germanium composite materials having unique optical properties, one being a complete photonic bandgap.

The synthesis and characterization of high quality, very large scale, face centered cubic photonic band gap (PBG) material comprising a composite of pure germanium and air is disclosed. Infiltration of these templates by germanium followed by removal of the silica provides inverse germanium opals. Two different methods of infiltration will be described:

Method (1): One of them consists of the infiltration of a germanium

alkoxide within the void lattice of a silica opal template. The alkoxide is later hydrolyzed to form germanium oxide. Then, the germanium oxide is reduced to germanium in a hydrogen atmosphere at high temperature. This process is performed in a cyclic way until the desired amount of germanium is infiltrated.

5 Method (2): The other infiltration method is the chemical vapor deposition of germanium into a self-assembling silica opal template.

In both cases, subsequent removal of the template gives rise to a germanium inverse opal.

10 The materials presented here show the highest periodic dielectric contrast ever achieved in the near infrared (NIR) region. This achievement opens a new door for complete control of radiative emission from atoms and molecules, light localization and the integration of micron scale photonic devices into a three-dimensional all-optical micro-chip.

15 More particularly, the present invention provides two different methods for the synthesis of a 0.1 mm to 1.0 cm scale single crystal of a face centered cubic (fcc) PBG material, comprising a close packed 1.0 –2.0 micron diameter air spheres in pure germanium. These germanium PBG materials show large reflection peaks in the NIR, resulting from the appearance of PBGs. The self-assembly synthetic approach that we employ is straightforward, mild,
20 inexpensive, accurate, and yields inverse opal structures made of germanium comprising up to 10,000 x 10,000 x 10,000 unit cells into which various defect network architectures can be imprinted during the initial stage of synthesis. The methodology is compatible with, and can be easily integrated into, existing germanium fabrication manufacturing facilities.

25 In one aspect of the invention there is provided a three dimensional periodic composite material comprising germanium and at least one other dielectric component having an effective dielectric constant smaller than the dielectric constant of germanium, the periodic composite material having a lattice periodicity ranging from about 1.0 microns to about 2.0 microns.

In another aspect of the invention there is provided an inverse germanium opal comprising close packed spherical air voids in germanium, the spherical air voids having a diameter in a range from about 1.0 to about 2.0 microns.

5 In another aspect of the invention there is provided a method of growing an inverse germanium opal, comprising:

providing a three dimensional opal template comprising particles having an effective geometry and composition;

infiltrating the opal template with an effective amount of germanium into voids between said particles; and

10 etching out the particles to produce an inverse germanium opal.

The present invention also provides a method of growing an inverse germanium opal, comprising:

providing a three dimensional silica opal template made of silica spheres;

15 infiltrating voids in the silica opal template with enough germanium to fill between about 50% to about 100% of said voids; and

etching the silica spheres out of the template to produce an inverse germanium opal.

20 The present invention also provides a method of growing an inverse germanium opal with a complete three dimensional photonic bandgap, comprising:

providing a three dimensional silica opal template including substantially mono-disperse silica spheres having a diameter in a range from about 1.0 to about 2.0 microns;

25 infiltrating voids in the silica opal template with enough germanium to fill between about 50% to about 100% of said voids; and

etching all the silica out of the template to produce an inverse germanium opal.

BRIEF DESCRIPTION OF THE DRAWINGS

The method of synthesis of germanium-based photonic band gap materials according to the present invention will now be described, by way of example only, reference being made to the accompanying drawings, in which:

5 Figure 1 shows a diagram of the cyclic process employed to infiltrate germanium in the void lattice of the silica opal template in accordance with the method number (1) of the present invention.

Figure 2 shows the PXRD pattern of the germanium infiltrated opal. The peaks observed correspond to the diamond like structure of bulk germanium.

10 Figure 3 is a scanning electron micrograph (SEM) of a (A) {111} and (B) {100} facets of a germanium infiltrated opal produced in accordance with the method number (1) of the present invention.

Figure 4 show SEM images of different types of internal fcc facets: (A) {100} (B) {110} and (C) {111} of a germanium inverse opal produced in accordance with the method number (1) of the present invention.

15 Figure 5 is a typical MicroRaman spectrum of the inverse opal. The Γ_{25} phonon of germanium can be clearly observed.

Figure 6 shows the reflectance spectrum of a germanium inverse opal with a $1.14 \mu\text{m}$ lattice parameter together with the corresponding photonic band. In this case, the composition of the photonic crystal is 85% air and 15% germanium. **Right:** Reflectivity spectrum of the fcc germanium structure shown in figure 3. Reflectivity was measured employing a microscope that concentrates the light in a $20 \times 20 \mu\text{m}^2$ spot, while the single crystal domain size is around $100 \times 100 \times 100 \mu\text{m}^3$. An exhaustive mapping of the sample was done, many different domains having been characterised. The microscope aperture determines a collection angle between 15° and 35° from normal incidence to the Γ -L direction. The two first stop bands correspond to the **Left:** Photonic band structure in Γ -L for our photonic crystal. It can be clearly seen that it presents three clear minima in the density of states (gaps) for those energy ranges within

the shaded areas. **Centre:** We have chosen the band structure along L-U to show the evolution of these gaps as we tilt the propagation direction with respect to the {111} axis, as it is the case in the experiments. This approximation is supported by the high symmetry of the fcc structure, since the photonic bands are nearly isotropic around the L point. We have established a correspondence between the wavevectors along L-U and the external incident angles. A rather good agreement is found between theory and experiment.

Figure 7 shows the calculated band structure of the germanium fcc lattice made of 15% germanium and 85% air. The shaded region shows the calculated positions of the complete photonic bandgap.

Figure 8 is a SEM image of a germanium infiltrated silica opal prepared using Method (2) having a lattice parameter of 1.7 microns.

Figure 9 is a low magnification SEM image of the germanium inverse opal (lattice parameter 1.7 microns) prepared using Method (2) showing the long range order in the resulting inverse opal.

Figure 10 shows an SEM image of a {110} face of the germanium fcc structure prepared using Method (2) wherein the large holes connecting the air spherical cavities reflects the strong sintering between silica spheres in the template.

Figure 11 shows a reflectance spectra of the germanium inverse opal in which only the electronic transparency region ($\lambda > 1.85$ microns) is shown.

Figure 12 shows a calculated complete photonic band structure for the germanium inverse opal shown in Figures 8-10 in which the full photonic band gap is highlighted.

DETAILED DESCRIPTION OF THE INVENTION

In a preferred embodiment of the present invention there is provided a three dimensional periodic composite material comprising germanium and a dielectric component having a dielectric constant smaller than the dielectric

constant of germanium. The periodic composite material has a cubic lattice periodicity (center to center distance between adjacent cubic repeating units) ranging from about 1.0 microns to about 2.0 microns.

5 In a more preferred embodiment the dielectric constant of the lower dielectric component is in a range from about 1 to about 2.1 and said composite material is characterized by at least one complete photonic bandgap centered in the range of 1.9 to 4.0 microns.

PREPARATION OF OPAL SUBSTRATE

10 A preferred method of producing this germanium/dielectric material composite involves producing an inverse germanium opal from a sintered silica opal with the silica opal produced using monodisperse silica spheres of selected diameter, which are ordered in an fcc lattice and sintered at a temperature between 1223 K and 1323 K to give them mechanical stability and control the
15 filling factor. Details of an exemplary, non-limiting method of fabrication of a silica opal are as follows.

After providing the spheres from which the opal is to be produced, the next step in the fabrication of an artificial opal is the crystallization of the silica spheres into a three dimensional periodic structure or template. The inventors
20 have discovered that different methods for settling silica spheres are needed depending on the sphere diameter.

EXAMPLE I

25 **Crystallisation Of Spheres Of Diameters Between 0.2 And 0.55 Microns In A Face Centred Cubic Structure**

In this range, natural sedimentation (under 1 gravity) in an aqueous solution was used to crystallize the opal. There was dispersed 175 mg of spheres in 180 cm³ of water. The silica spheres were allowed to settle on a
30 circular polished poly(methylacrylate) substrate (mean rugosity < 50 nm) having

a 2 cm diameter. The sediment was completely formed after several days, depending on sphere size (larger spheres sedimented faster than the smaller ones). Once the sediment was formed, the supernatant liquid was removed and the sedimentation tube placed in an oven at 60°C until the water was fully
5 evaporated. Afterwards, the sediment was carefully removed from the substrate and its structure was analyzed.

Studies of the growing surface confirmed that the spheres arrange in a close packed structure, which grows close to the equilibrium following the Edwards-Wilkinson equation. This implies the particles behave as effective hard
10 spheres. This conclusion is supported by the fact that no ordering was observed in the suspension even at high concentrations. Also, the sedimentation velocity followed Stokes law. Three-dimensional order was analysed by SEM and optical transmission spectroscopy. Samples were fractured and the internal free surfaces observed. Cleft edges show long range face centred cubic domains, no
15 facets belonging to any other type of periodic structure being observable. Domain size ranges from 20 to >100 microns.

EXAMPLE 2

i) Crystallization Of 0.448 ± 0.006 Micron Diameter Silica Spheres

20 Initially 175 mg of such spheres were dispersed in 180 cm³ of double distilled water. Spheres were let to settle during 7 days on the mentioned above substrate. The supernatant liquid was then removed until a 2 mm high liquid column was left above the sediment. The sedimentation tube was then placed in an oven at 60°C until the whole liquid evaporated (1 day). The sediment was
25 then carefully removed from the substrate and its internal structure analyzed.

ii) Crystallisation Of Spheres Of Diameters Between 0.55 And 1.3 Microns In A Face Centred Cubic Structure By Using Different Solvents, Co-solvents And Temperatures

5 In order to obtain opals made of large spheres different organic solvents were employed as a sedimentation medium. This was done to change the falling velocity of the particles as well as the interactions between them. Ethyleneglycol, glycerol, acetone and ethanol and their aqueous mixtures at several different concentrations were used as settling media. Spheres were then allowed to
10 settle. When the sediment was formed, the supernatant liquid was removed until a 2 mm height liquid column was left in the sedimentation tube. Then, the sediment was dried at different temperatures in an oven, ranging between 60°C and 120°C. Temperature plays an important role in the crystallization process. Excellent results were obtained. SEM and optical characterization show that fcc
15 optical quality opals were obtained by this procedure.

EXAMPLE 3

i) Crystallization Of 0.853 ± 0.012 Microns Diameter Silica Spheres.

 About 179 mg of spheres having a diameter of 0.853 ± 0.012 microns were
20 dispersed in 180 cm³ of a mixture of 40% weight of ethyleneglycol and 60% of double distilled water. Spheres were allowed to settle during 4 days on the above mentioned substrate. Then the supernatant liquid was removed until a 2 mm height liquid column was left above the sediment. The sedimentation tube was then placed in an oven at 60°C during 1 day and later at 100°C during 5
25 days. When the sediment was dry, it was carefully removed from the substrate and its internal structure analyzed. Scanning electron micrographs demonstrated long range fcc domains were present (data not shown).

30

ii) Crystallisation Of Spheres Of Diameters Between 0.55 And 0.9 Microns In A Face Centred Cubic Structure By Electrophoretic Deposition To Control Artificial Opal Growth

5 Natural sedimentation presents two problems. The first one is the time required to obtain an opal. If the silica spheres are too small (under 0.30 microns of diameter), several weeks are needed or even they may not settle at all because thermal agitation compensates gravitational forces. The other difficulty that has been observed is related to heavy spheres which are over 0.56 microns
10 in diameter. In this case the sedimentation velocity is such that it is difficult to achieve an ordered array and it becomes completely impossible if the diameter is further increased. In this situation, the electrophoretic phenomena offers a method for overcoming these two problems. Using the electric field to drive the sedimentation velocity and keep it around 0.4 mm/hour would solve the
15 difficulties mentioned before. The model of constant velocity particle packing is based on the interaction of gravitational ($F_g = 1/6\pi\rho_s g d^3$), Archimedes ($F_A = 1/6\pi\rho_w g d^3$) and frictional forces ($F_f = 3\pi\eta v d$). Where ρ_s and ρ_w are the spheres and water mass densities, g is the gravity acceleration, η is the viscosity of water, d is the spheres diameter and v is their velocity. When all forces are
20 balanced, the Stokes law is obtained.

It is well known that SiO_2 particles in a colloidal suspension have a surface charge density when they are away from the point of zero charge (PZC), in which case the electric charge is null. Taking into consideration the force produced by an electric field E parallel to all other forces, the following equation
25 is obtained for the velocity:

$$v = [(d^2 (\rho_s - \rho_w)g)/18\eta] + uE$$

where the first part of this equation is the classical Stokes law and the second part corresponds to the contribution of the electric field to the sedimentation velocity, related to the mobility of the spheres u . Now, the main problem is how
30 to calculate the particle's mobility. The application of the electrophoretic concept

can solve it. Provided that Stokes velocity without electric field is calculated with great accuracy, the electrophoretic mobility can be obtained in a straightforward manner if Stokes velocity is subtracted from the experimental velocity of the sample under a known electric field. Once the mobility is determined, the electric field necessary to achieve a given velocity can be stated beforehand.

The electrophoresis cell comprised a cylindrical tube (2 cm of diameter) of poly(methylacrylate) fixed to the base where the opal should settle, obtained from a standard silicon wafer sputtered with titanium or gold (with less than 0.1 nm of rugosity and thick enough to assure a good conductivity). The material used for the upper electrodes were platinum because it has the highest redox potential so that electrolysis is avoided. Both electrodes are connected to a dc source in order to develop an electrical field. With this method sediments with thickness ranging between a few monolayers and 1 mm (depending on the amount of silica spheres used) with surface areas about 3.1 cm² are produced. To measure the sedimentation velocity, the height descended by the colloid/clear water interface (setting 0 mm the initial height) was monitored with time.

The electrophoretically assisted sedimentation of SiO₂ spheres was studied. An electric field was applied to colloidal suspensions of SiO₂ spheres in which the original pH was varied by adding HCl to change the surface charge. The point of zero charge, PZC, of silica occurs at a pH=2.5, so the pH values of the suspensions were chosen to be different enough without being close to the PZC: pH=3.8 and the reference value (no acid added) of pH=8.4. The results of the sedimentation velocities for silica spheres of 0.50 microns of diameter are graphically compared with the theoretical Stokes fall of a sample without electric field in the left panel of Figure 6. It can be clearly seen that, as the pH moves away from the PZC, the mobility increases and so does uE .

In order to study the effects of velocity variations on silica particle ordering, two more sedimentations were prepared from the same sample. One of

the suspensions was left to settle in the absence of an electric field, whereas in the other one the electrodes were inverted to decrease the sedimentation velocity by opposing the gravity and the electric field. Since the mobility can be extracted from the previous experiment ($u = -3.9 \mu\text{m cm/V}$), the electric field needed to get the desired velocity (0.4 mm/hour) was calculated to be 0.5 V/m. The experimental value ($v = 0.35 \text{ mm/hour}$) was close to it. In Table 4 the results from this experiments are numerically compared.

Table 4. Mobilities and velocities from SiO_2 spheres of 0.50 microns in diameter at different pH and electric fields.

pH	E (V/m)	u ($\mu\text{m cm/V s}$)	v (mm/h)
3.8	-33	-2.0	2.9
8.4	-33	-3.9	5.2
8.4	0.5	-3.9	0.35

Electronic and optical microscopy studies of all these samples were made and it was observed that the sample in which sedimentation was slowed electrophoretically demonstrated superior ordering than the one settled in the absence of an electric field and while the accelerated samples from the previous experiment presented no order at all. Bragg diffraction was performed as well showing that the opal grown with controlled sedimentation presented well-defined Bragg peaks.

For comparison, silica spheres with a diameter of 0.87 microns were settled both in the presence and absence of an electric field. A high velocity (1.54 mm/hour) was obtained for these large spheres and no long-range order was achieved as evidence by the Fourier transformed image (not shown). A colloidal suspension of silica spheres of the same diameter was settled under a retarding electric field, in which the velocity was kept close to 0.35 mm/hour and

large ordered domains were obtained when sedimentation was performed under an appropriate electric field. Confirmation of this is evident from the Fourier transforms of both images, the opal settled under electric field presents a clear pattern that is not present in the naturally settled opal.

5 A Bragg diffraction study from the opal grown under slowed sedimentation conditions was performed after sintering and very clear peaks were observed while the other sample did not present any kind of peak as a result of the lack of large enough ordered domains. In addition, a little percentage of small spheres was present in this sample. They were observed in SEM images of the naturally
10 settled sample but they were not present in the other one because the electric force compensated the gravity force. This suggests that the electrophoretic concept could be used to control the presence of small spheres in sedimentation when monodispersity is not granted.

 Normally a suspension containing silica spheres of small diameter, (e.g.
15 0.205 microns of diameter) would take up to two months to settle to produce the sediment. The settling rate using electrophoretic assisted sedimentation was accelerated from 0.09 mm/hour (natural velocity) to 0.35 mm/hour so that complete sedimentation was achieved in less than two weeks without decreasing the optical quality. Diffraction studies of the as-grown opal showed Bragg peaks
20 which denoted the presence of order within the opal.

 The results disclosed herein demonstrate the importance of using electrophoretic deposition for opal sedimentation. With this method it is possible to assemble opals comprising ordered arrays of spheres with diameters greater than 0.55 microns which has heretofore been a major limitation. Electrophoretic
25 assisted deposition has been shown to be an efficient way to control the sedimentation velocity of silica spheres over a wide range of diameters.

EXAMPLE 4

300 mg of SiO_2 spheres with a diameter of 0.87 microns were suspended in 30 ml of double distilled water. An electric field value of $E = -8.3 \text{ V/m}$ was applied across a column of 8 cms in height containing the suspension. The sedimentation velocity was 0.35 mm/hour, and the mobility of these spheres was 4.0 mm cm/Vs. Six days were needed to perform the whole sedimentation and two more days to dry the samples at 60°C in an oven.

Sintering The Three dimensional Periodic Silica Opal

Crystalline sediments of silica spheres suffer from low mechanical stability which makes them difficult to handle. In order to solve this, as-grown samples were sintered at different final temperatures. The sintering process leads to the necking, or the formation of small necks, between neighboring silica spheres. Necking is the thermally induced softening and flow of silica into the regions defined by the touching of silica spheres in the colloidal silica crystal to create a silica neck with a diameter that facilitates infiltration of silicon into the voids of the silica opal and etching of silica from the infiltrated opal to create the inverse silicon opal.

Another extremely important parameter of the opals when used as matrices for other compounds, is the filling fraction (ratio between the volume occupied for each compound and the total volume of the structure). Sintering provides an accurate way to control the filling fraction between 74% and 100% of silica in opals. The process of necking allows tuning of the dimensions of the silica opal and the resulting inverse silicon opal. The process of necking also provides mechanical stability to the template in addition to providing a control over the opal void volume for subsequent synthesis and providing the connected network topology for removal of the template by an etching process. Studies have shown that silica opals sintered at 950°C for 3 hours have a mechanically stabilized compact face centered cubic (fcc) structure with a silica filling factor of

74%. Further, sintering the opals at different temperatures between 950°C and 1100°C for different periods of time provided a method of controlling or tuning the optical properties and the free volume in the opals.

5 Example 5 below provides an illustrative, non-limiting example of use of sintering temperature for tuning the optical and physical properties of a silica opal.

EXAMPLE 5

10 Pieces of an opal synthesized from 0.426 micron diameter spheres were sintered at 1025°C for different periods of time. One piece of the opal was placed in an oven and heated up to 70°C employing a temperature gradient of 1°/min. Once the temperature reached 70°C it was kept constant at 70°C for 3 hours to prevent rapid or abrupt water de-sorption from the opal. After this, the temperature was increased up to 1025°C employing a temperature gradient of 1°/min. The opal was maintained at this temperature for 3 hours. Two other 15 pieces of the starting opal were sintered using the same procedure but one piece was sintered for 6 hours and the other for 12 hours. Characterization of the optical properties of the differently sintered opals reveal the free volume of the three opal pieces were different, decreasing with increasing temperature.

20

INFILTRATION OF SILICA SUBSTRATES WITH GERMANIUM

The present method provides two non-limiting methods of producing germanium based photonic crystals. Figures 1 to 7 relate to method (1), with the example being fabrication of a photonic crystal having a germanium inverse opal 25 structure with a 1.14 microns lattice parameter for the opal. Figures 8 to 12 relates to method (2) for producing a photonic crystal based on a germanium inverse opal with a 1.7 micron lattice parameter of the opal. A major advantage obtained by producing an inverse germanium opal in accordance with the present invention is that composites with complete photonic bandgaps can be

economically synthesized which heretofore has not been realized.

1) Fabrication of a Germanium Inverse Opal Using Method (1)

Method (1): Germanium (Ge) was grown inside the void spaces of the silica opal template using tetramethoxyorthogermanate (99% purity $\text{Ge}(\text{OCH}_3)_4$, TMOG) liquid as a precursor, which easily infiltrates porous silica. TMOG infiltration takes place at room temperature. Once the silica opal template is fully infiltrated, TMOG is hydrolyzed to form germanium oxide (GeO_2) within the spaces between spheres. Once the GeO_2 is formed, it was reduced to Ge at a temperature of 823 K and in hydrogen (H_2) atmosphere. The GeO_2 may be reduced in a range of temperatures.

This process is repeated until a good connectivity of the Ge guest lattice is attained. When this is achieved, the silica of the matrix is removed and an inverse germanium opal is obtained. Example 1 below provides illustrative, non-limiting examples of use of germanium infiltration into the silica opal template and etching of the silica template.

While tetramethoxyorthogermanate is a preferred material for infiltration into the opal template, it will be understood that other liquid or aqueous/non-aqueous solution phase germanium-based reagents, which can be hydrolyzed and/or calcined in air-or oxygen through to germanium dioxide and then reduced to germanium could also be used. Examples include, but are not limited to, germanium glycolates, germanium halides, alkylgermaniumhalides, alkylgermaniums all of which may be converted to germanium dioxide by some combination of the aforementioned hydrolysis and calcination in air or oxygen after in-filling of the opal. Also many simple germanium salts like nitrates, acetates, sulfates, oxalates under solution phase basic conditions are contemplated to hydrolyze and calcine in air or oxygen through to germanium oxides. Also, any of the above routes may be tailored to produce colloidal dimension germanium dioxide that can directly be impregnated into the silica opal template.

EXAMPLE 6

First, the sintered silica opal was placed in a hermetically sealed cell in which vacuum (10^{-2} torr) was made. In this way, the whole pore volume in the opal was available to subsequently infiltrated materials; hence, a complete and homogeneous infiltration was possible. The template was then embedded in TMOG, which was injected in the cell. The alkoxide was allowed to impregnate the bare opal. At that moment, the infiltrated opal became translucent as a consequence of the dielectric constant matching that took place when TMOG (dielectric constant $\epsilon = 1.96$) filled all the empty volume of the matrix ($\epsilon = 2.1$).

The infiltration of metal alkoxides has been used to obtain inverse opals of several metal oxide compounds (see B. T. Holland, C. F. Blanford and A. Stein, *Science* 281, 538 (1998); J. Wijnhoven and W. L. Vos, *Science* 281, 802 (1998)).

Second, TMOG was hydrolyzed at room temperature by flowing a mixture of N_2 and H_2O vapor, which gave rise to GeO_2 formation in the opal lattice. The remaining methanol, product of the hydrolysis reaction, was removed by pumping the reactor. At this point, Ge^0 was formed from GeO_2 by direct reduction in H_2 atmosphere at 823 K. In order to completely fill the interparticle volume and, consequently, to assure the connectivity of the germanium lattice, the opal was subjected to five rounds of the GeO_2 and Ge formation processes just described. Figure 1 shows a diagram of the cyclic process employed.

Finally, the Ge infiltrated opal was chemically etched in a 1 wt. % hydrofluoric acid in water solution. In this way the SiO_2 spheres of the matrix were removed to obtain Ge inverse opals. Template sintering was responsible for the formation of necks between the SiO_2 spheres, a treatment which not only conferred robustness to the structure but also allowed the HF solution to flow through the whole structure as the SiO_2 was being removed.

Characterization of the Germanium Infiltrated Opal

X-ray diffraction (XRD) of the germanium infiltrated opal (five infiltration

cycles) indicated that the synthesized germanium was crystalline. The XRD pattern is shown in Figure 2. SEM characterization of the internal facets showed that a good connectivity of the germanium guest lattice is achieved after five cycles. This can be seen in Figure 3. A thick layer of the opal template is present and a homogeneous and high degree of infiltration.

Characterization of the Germanium Inverse Opal

A detailed structural study of the 3D order of the structures resulting of the chemical etching was made. Etched samples were carefully cleaved and studied by SEM. Chemical analysis performed by EDX allows us to check that the matrix is efficiently eliminated by the soft HF attack without damaging the guest material. No silica was detected deep inside the acid treated sample.

Facets consistent with a fcc arrangement of air spheres are apparent in the fractured edges. The Ge obtained from GeO_2 shows a tendency to form a mesh, rather than an array of interconnected shells coating the spheres. This is clear on inspection of the SEM pictures of Figure 4, in which front views from the main crystal directions ($\{100\}$, $\{110\}$ and $\{111\}$) are displayed. This disposition could have its origin in the large energy needed to get a contact surface between Ge and oxides (see Tomsia, A. P.; Saiz, E.; Dalgleish, B. J.; Cannon, M. **Proceedings of the 4th Japan International SAMPE Symposium**; September 25-28, 1995). This tendency implies that no additional air voids appear between the hollow spheres after SiO_2 etching, as can happen when chemical vapor deposition processes are employed to synthesize materials in the opal void lattice. The repeated cycle of synthesis with aggregation of crystals during the reduction process furnishes the germanium that is formed within the bare opal with a high connectivity in a thick layer of the template. This provided, the germanium lattice does not collapse on dilution of the silica matrix in spite of being a highly open structure. Therefore, the long range fcc order inherited from the template is preserved in the Ge inverse opals.

In addition Micro-Raman spectroscopy (MRS) was used to ascertain that

the germanium quality was preserved after the soft acid etching. Many different areas of the cleft edges were analyzed. The germanium phonon peak was observed everywhere in the inverse opal samples and it was narrow and centered at 296 cm^{-1} , confirming the presence of crystalline germanium (see Figure 5).

The optical feature of a macro-porous germanium fcc structure presenting a $1.14\text{ }\mu\text{m}$ lattice parameter was measured by focusing white light in a $20\times 20\text{ }\mu\text{m}$ spot on a single domain. The experimental set-up determines that radiation propagates close to the Γ -L direction inside the crystal. The reflectivity spectrum obtained is shown in figure 6. Photonic band structure calculations based on the plane wave method are also shown. The best fit was achieved assuming a mesh of germanium occupying 15.6% of the whole volume. We only show the band structure along directions that are relevant for understanding the experiments (Γ -L and L-U).

Three clear peaks can be observed in the spectrum. They correspond to different minima in the photonic local density of states (DOS) around the L point, as can be seen in the calculation. Shaded areas indicate where the three forbidden energy bands are expected, showing quite a good agreement with the experimental results. The peak at lower energy (0.60 eV) appears in the transparent region of bulk germanium. It corresponds to the first non-complete stop band, as can be seen in the band structure, since it vary with the propagation direction. The indirect and direct electronic band gaps are placed at 0.67 eV and 0.79 eV respectively. So, the second peak in the reflectance, corresponding to the second stop frequency photonic band is above the indirect electronic gap and close to the direct one. The small peak observable around 1 eV falls deep inside the Ge absorption region, above both electronic band gaps. This peak presents a 12% gap width to midgap ratio and must correspond to the full PBG (predicted by Sözüer, H.S., Haus, J.W. & Inguva, R. **Phys. Rev. B** **45**, 13962-13972 (1993); Busch, K. & John, S. **Phys. Rev. E** **58**, 3896 (1998)). Its

low intensity is due to the fact that the gap appears in the germanium electronic absorption region.

These results show the optical quality of a structure made of fcc ordered micrometer cavities in a germanium matrix. It presents the highest dielectric contrast ($\epsilon_{\text{Ge}}/\epsilon_{\text{air}}=16$) ever achieved in an electronically transparent material in the NIR region. Such a huge dielectric contrast has been previously unattainable in other periodic macroporous materials. As a result of these features, several different energy bands in the near infrared region are not allowed to propagate through the photonic crystal.

The synthesis of a very large scale, germanium based PBG material offers a number of imminent possibilities, involving further infiltration of this highly open structure with liquid crystals, which may lead to tunable full PBG materials.

Fabrication of a Germanium Inverse Opal Using Method (2)

Germanium is grown inside the voids of the template by chemical vapor deposition (CVD) preferably using a mixture of 20% digermane (Ge_2H_6) gas and 80% hydrogen (H_2) gas as a precursor. The template is placed in a quartz vessel and evacuated using a vacuum pump to about 5×10^{-6} torr. The digermane/hydrogen gas mixture is added to the vessel. The vessel is heated for varying times and temperatures to obtain samples with different degrees of infiltration. The vessel is then evacuated using a vacuum pump to removed unreacted digermane and hydrogen.

As deposited, the germanium is in the form of amorphous hydrogenated germanium. Heating of the sample drives off the hydrogen to form amorphous germanium. The sample can be heated further to form polycrystalline germanium. Typically the samples are annealed at 500°C in order to improve the germanium crystallinity and to allow diffusion of germanium inside the void structure.

The pressure, temperature and time of reaction can be varied as

summarized in Table 1:

Table 1

	<u>Heating Profile</u>	<u>Pressure</u>
5	5 hours at 300°C	200 torr
	2 hours at 300°C	500 torr
	5 hours at 200°C, followed by 4 hours at 300°C	200 torr
	21 hours at 300°C	930 torr
	21 hours at 200°C	290 torr
10	21 hours at 300°C	660 torr
	21 hours at 250°C	490 torr
	from 25 °C to 500°C over 10 hours, followed by 2 hours at 500°C	180 torr

Besides using digermane, it will be appreciated that other volatile germanium-based reagents could also be used like, but not limited to, germanium halides, alkylgermaniumhydrides, alkylgermaniumhalides, alkylgermaniums, germaniumacetylacetonates all typically used in the presence of hydrogen.

Example 2 below provides illustrative, non-limiting examples of use of germanium infiltration into the silica opal template and annealing of the germanium in the template using this method.

EXAMPLE 7

Growth of a Germanium Inverse Opal with a Lattice Parameter of 1.7 Microns.

In this example, we start from a bare opal made of silica spheres arranged in a face centered cubic structure whose lattice parameter is 1.7 microns. It was previously sintered at a temperature of 1223 K to form necks

between the spheres. First, the template is introduced in the reactor and it is pumped until a pressure of 5×10^{-6} torr is achieved. The reactor is cooled, by using liquid nitrogen as the cryogen. Second, the 20% digermane in hydrogen gas mixture is allowed to fill the vacuum system and reach the sample. The low
5 temperature (77 K) of the reactor gives rise to the condensation of the Ge_2H_6 inside it.

Afterwards the reactor was warmed up to room temperature and introduced into an oven. Then, it was heated up to 573 K and kept at this temperature for 21 hours. Then, it was cooled down to room temperature. An
10 analysis of the sample structure performed by scanning electron microscopy (SEM) reveals that the growth takes place layer-by-layer, which gives rise to a uniform shell coating the silica spheres (Figure 8). This treatment also allows a uniform infiltration throughout the whole silica opal template. By measuring the coating thickness (around 75 nm) and the degree of sintering of the sample, we
15 can estimate that the 63% of the pore volume of the silica template has been infiltrated.

The germanium infiltrated sample, was later etched by immersing it in a 1% HF solution for 48 hours. The sample was previously cut into pieces to favor the penetration of the solution into the silica/germanium composite opal. By this
20 procedure, we obtain a germanium inverse opal which has inherited the long-range order of the original template, as can be seen in Figure 9. A careful inspection of the cleaved edges of the sample permits us to see different crystalline planes of the germanium face centered cubic structure. A {110} face is shown in Figure 10.

25 The optical properties of the germanium inverse opal are measured in reflection mode. The reflectance spectrum (see Figure 11) shows clear peaks that reveal the optical quality of the material and confirms its photonic band gap behavior. Several measurements were taken focusing the incident beam in different areas of the sample surface. These confirm the homogeneous

infiltration in the whole template and the uniformity of the germanium layer coating the spheres.

A detailed analysis of these optical properties was performed, by using photonic band structure calculations. On the basis of the data obtained from the SEM characterization (lattice parameter, coating thickness and degree of sintering), we find a good agreement between theory and experiment concerning the number of peaks observed and their position. The calculation indicates that the peak observed at 2.15 microns should be a full photonic band gap. This can be seen in the corresponding complete photonic band structure diagram shown in Figure 12.

The method of producing the periodic silicon-air composites starting with silica opals and producing the inverse opals therefrom is a preferred or best mode known at present since the periodicity of the opal can be efficiently transferred to the inverse opal. However, those skilled in the art will appreciate that synthesis of periodic silicon-air composites or variants thereof as disclosed herein will not be restricted to conversion of silica opals. Other silica templates and non-silica templates may be employed. Silica templates involving lattice structures other than the close packed face center cubic lattice may be used and templates using two or more different sphere sizes may be used. These include for example the hexagonal close packed structure, the body center cubic structure, the diamond lattice structure, the hexagonal AB_2 structure. Non-silica templates include periodically arrayed block co-polymers and other self-assembling organic materials. In this case non-spherical, repeating units can be realized. Here a multi-stage infiltration process is required since the polymeric material may not withstand the high temperatures required for silicon CVD. Therefore, a material such as silica would be infiltrated into the polymer template and the polymer template will be removed, prior to the final infiltration with silicon and the final removal of silica.

Those skilled in the art will understand that germanium photonic crystals

grown by the present method may not have a complete PBG but only a photonic pseudo-gap, that is to say a material for which there is a large suppression in the total photon density of states (DOS) from what it would be in either air or in bulk silicon, have important applications as well. From theoretical studies (see S.

5 John and T. Quang, **Physical Review Letters** 78, 1888 (1997)), it is known that even a sharp drop in the DOS by a factor of 2 over a small frequency range

would lead to novel optical switching devices. The same holds true for materials grown by the present method, which do not exhibit a complete photonic band

gap in the total density of states, but only a complete photonic band gap in the

10 local photon density of states. In particular, the local density of states (LDOS) controls the rate of spontaneous emission of light from atoms and molecules at particular locations in the photonic crystal, for lasing and optical switching applications. The pseudogap material encompasses a broader range of

materials and composites than the rather restricted set of materials which exhibit

15 a complete PBG. Likewise, materials with a complete gap or pseudogap in the LDOS encompass an even broader range of materials than those which exhibit corresponding gaps in the total density of states.

The LDOS is the density of states as felt by an atom or molecule in a particular position in the photonic crystal. As stated above, a gap in the LDOS
20 may occur under less restrictive conditions than those required for a gap in the total DOS. For microlaser device applications, it is contemplated that low threshold laser action may be achieved with a gap only in the LDOS where the light emitting atoms are actually situated. The LDOS is what actually controls the radiative dynamics of individual atoms and molecules. Finally, it should be noted
25 that whereas the total DOS may only have a gap of only 10% in a silicon inverse opal with a "complete 3-d PBG", the LDOS may exhibit a gap of up to 20% in the same material.

Certain germanium-air composites comprising doped germanium are useful as sensors. The germanium may be doped n-type by doping with

phosphorus or p-type obtained by doping with boron. The dopant is incorporated by infiltrating the germanium in the presence of gaseous phosphenes or boranes. Such a three dimensional periodic composite material comprising germanium and a dielectric component having a dielectric constant small than a dielectric constant of germanium is treated by anodic oxidation to render it luminescent. The doped macroporous germanium crystal with controlled porosity germanium walls functions as a chemoselective sensor to discriminate optically between molecules in a mixture, depending on the diameter of the pores that are grown in the germanium walls.

The foregoing description of the preferred embodiments of the invention has been presented to illustrate the principles of the invention and not to limit the invention to the particular embodiment illustrated. It is intended that the scope of the invention be defined by all of the embodiments encompassed within the following claims and their equivalents.

THEREFORE WHAT IS CLAIMED IS:

1. A three dimensional periodic composite material comprising germanium and at least one other dielectric component having an effective dielectric constant smaller than the dielectric constant of germanium, the periodic composite material having a lattice periodicity ranging from about 1.0 microns to about 2.0 microns.
2. The periodic composite material according to claim 1 having a face centered cubic lattice periodicity.
3. The periodic composite material according to claim 1 wherein said composite material is characterized by at least one pseudo-photonic band gap in the local photon density of states.
4. The periodic composite material according to claims 1 or 2 wherein said composite material is characterized by at least one pseudo-photonic band gap in the total photon density of states.
5. The periodic composite material according to claims 1 or 2 wherein said composite material has at least one complete photonic band gap in the local photon density of states.
6. The periodic composite material according to claims 1 or 2 wherein the lower dielectric constant material has a dielectric constant is in a range from about $\epsilon=1.0$ to about $\epsilon=2.2$ and said complete photonic band gap is located in the total photon density of states.
7. The periodic composite material according to claims 1 or 2 wherein said

composite material is characterized by at least one complete photonic band gap in the total photon density of states spanning at least 5% of a center frequency of the photonic band gap.

8. The periodic composite material according to claim 3 wherein a ratio of said complete photonic band gap to a center frequency in the local density of states ranges from 0% to about 25%.

9. The periodic composite material according to claims 1, 2, 3, 4, 5, 6, 7 or 8 wherein said dielectric component includes a silica-air or a germanium-air composite material.

10. The periodic composite material according to claim 4 wherein said low dielectric component is vacuum.

11. The periodic composite material according to claim 6 wherein said low dielectric component is air.

12. The periodic composite material according to claims 1, 2, 3, 4, 5, 8, 9, 10 or 11 wherein said periodic composite material is an inverse germanium opal.

13. The periodic composite material according to claim 12 wherein said complete photonic bandgap is centered on a wavelength in a range of about 2.0 to about 4.0 microns.

14. The periodic composite material according to claims 6, 7 or 11 wherein said complete photonic bandgap is adjustable by adjusting germanium to air ratio in said composite material.

15. The periodic composite material according to claims 1 to 14 wherein said germanium is selected from the group consisting of single crystal germanium, amorphous germanium, polycrystalline germanium, porous germanium and nanocrystalline germanium.

16. The periodic composite material according to claims 1 to 14 having dimensions in a range from $2 \times 2 \times 2$ unit cells to $a \times b \times c$ unit cells, wherein $2 < a < 10,000$, $2 < b < 10,000$, $2 < c < 10,000$.

17. The periodic composite material according to claims 1 to 14 having a planar thin film geometry with dimensions in a range from $1 \times 10 \times 10$ unit cells to $a \times b \times c$ unit cells, wherein $1 < a < 100$, $10 < b$, $c < 100,000$.

18. The periodic composite material according to claims 1 to 17 wherein said germanium includes a germanium alloy.

19. The periodic composite material according to claims 1 to 17 wherein said germanium contains dopants, said dopants including magnetically sensitive dopants, electrically sensitive dopants and optically sensitive dopants.

20. The periodic composite material according to claim 19 wherein said doped germanium is selected from the group consisting of n-type germanium wherein said electrically sensitive dopant is phosphorous and p-type germanium wherein said electrically sensitive dopant is boron.

21. The periodic composite material according to claim 18 wherein said germanium alloy is selected from the group consisting of germanium-carbide

alloys $\text{Ge}_x\text{C}_{1-x}$, $0 < x < 1$, germanium-tungsten alloys, germanium-nickel alloys, germanium-titanium alloys, germanium-chromium alloys, germanium-aluminum alloys and germanium-molybdenum alloys.

22. The periodic composite material according to claim 19 wherein said optically sensitive dopants luminescence in a wavelength range substantially located in or near said photonic bandgap.

23. The periodic composite material according to claim 22 wherein said dopants emit light in a wavelength range from about 1.9 microns to about 4.0 microns.

24. The periodic composite material according to claim 23 wherein said dopants are selected from the group consisting of rare earth atoms, organic dyes, inorganic dyes, organic polymers and inorganic polymers.

25. The periodic composite material according to claims 1 to 24 wherein said germanium includes optically sensitive molecules adsorbed or chemically bonded to a surface thereof.

26. The periodic composite material according to claim 25 wherein said optically sensitive molecules includes one of luminescent dyes and luminescent polymers.

27. The periodic composite material according to claims 1 to 24 wherein said germanium includes hydrophilic or hydrophobic molecules adsorbed or chemically bonded to a surface thereof.

28. The periodic composite material according to claim 1 having a hexagonal close-packed or body centered cubic lattice periodicity.

29. An inverse germanium opal comprising close packed spherical air voids in germanium, the spherical air voids having a diameter in a range from about 1.0 to about 2.0 microns.

30. The inverse germanium opal according to claim 29 characterized by a complete photonic bandgap centered on a wavelength in a range from about 1.9 to about 4.0 microns.

31. The germanium opal according to claims 29 or 30 characterized by a complete photonic bandgap with a width to center frequency ratio in a range of 0 to about 15%.

32. The inverse germanium opal according to claims 29, 30 or 31 wherein said germanium is selected from the group consisting of single crystal germanium, polycrystalline germanium, nanocrystalline germanium, porous germanium and amorphous germanium.

33. The inverse germanium opal according to claims 29, 30, 31 or 32 having dimensions in a range from $2 \times 2 \times 2$ unit cells to $a \times b \times c$ unit cells, wherein $2 < a < 10,000$, $2 < b < 10,000$, $2 < c < 10,000$.

34. The inverse germanium opal according to claims 29, 30, 31 or 32 having a planar thin film geometry with dimensions in a range from $1 \times 10 \times 10$ unit cells to $a \times b \times c$ unit cells, wherein $1 < a < 100$, $10 < b$, $c < 100,000$.

35. A method of growing an inverse germanium opal, comprising:
- providing a three dimensional opal template comprising particles having an effective geometry and composition;
 - infiltrating the opal template with an effective amount of germanium into voids between said particles; and
 - etching out the particles to produce an inverse germanium opal.
36. The method according to claim 35 wherein said particles are substantially spherical particles in a face centered cubic lattice and the amount of germanium infiltrated is enough to fill between about 50% to about 100% of said voids.
37. The method according to claim 36 wherein said spherical particles are silica spheres.
38. The method according to claim 37 wherein said silica spheres are monodisperse and have a diameter in a range from about 1.0 to about 2.0 microns.
39. The method according to claims 35, 36, 37 or 38 wherein said opal template is infiltrated with enough germanium to fill about 90% to about 100% of said voids.
40. The method according to claims 36, 37, 38 or 39 wherein after infiltrating the opal template with germanium the infiltrated template is annealed to assist diffusion of germanium into said voids in the template.
41. The method according to claims 36, 37, 38, 39 or 40 wherein the three dimensional template has dimensions in a range from 2 x 2 x 2 unit cells to a x b

x c unit cells, wherein $2 < a < 10,000$, $2 < b < 10,000$, $2 < c < 10,000$.

42. The method according to claims 36, 37, 38, 39, 40 or 41 having a planar thin film geometry with dimensions in a range from $1 \times 10 \times 10$ unit cells to $a \times b \times c$ unit cells, wherein $1 < a < 100$, $10 < b$, $c < 100,000$.

43. A method of growing an inverse germanium opal, comprising:
providing a three dimensional silica opal template made of silica spheres;
infiltrating voids in the silica opal template with enough germanium to fill between about 50% to about 100% of said voids; and
etching the silica spheres out of the template to produce an inverse germanium opal.

44. The method according to claim 43 wherein the silica spheres are substantially monodisperse having a diameter in a range from about 1.0 to about 2.0 microns.

45. The method according to claims 43 or 44 wherein the silica opal template is infiltrated by chemical vapor deposition using a gaseous germane-hydride based precursor $\text{Ge}_n\text{H}_{2n+2}$ wherein $n=1, 2, 3, \dots$.

46. The method according to claims 43, 44 or 45 wherein the silica opal template is infiltrated by chemical vapor deposition using digermane (Ge_2H_6) gas as a precursor.

47. The method according to claims 43, 44 or 45 wherein the silica opal template is infiltrated by chemical vapor deposition using a volatile germanium-

based compound selected from the group consisting of germanium halides, alkylgermaniumhydrides, alkylgermaniumhalides, alkylgermaniums and germaniumacetylacetonates.

48. The method according to claims 43, 44, 45, 46 or 47 wherein during infiltration of germanium into the silica opal template a temperature of the template is maintained in a range from about 100°C to about 500°C.

49. The method according to claim 48 wherein the range is from about 250°C to about 350°C.

50. The method according to claims 43, 44, 45, 46, 47, 48 or 49 wherein after infiltrating the silica opal template with germanium the infiltrated template is annealed to assist diffusion of germanium into the voids in the template.

51. The method according to claims 43, 44, 45, 46, 47, 48, 49 or 50 wherein the three dimensional template has dimensions in a range from 2 x 2 x 2 unit cells to a x b x c unit cells, wherein $2 < a < 10,000$, $2 < b < 10,000$, $2 < c < 10,000$.

52. The method according to claims 43, 44, 45, 46, 47, 48, 49 or 50 having a planar thin film geometry with dimensions in a range from 1 x 10 x 10 unit cells to a x b x c unit cells, wherein $1 < a < 100$, $10 < b$, $c < 100,000$.

53. The method according to claims 43, 44, 45, 46, 47, 48, 49, 50, 51 or 52 wherein the silica is chemically etched using a fluoride-based etching medium.

54. The method according to claim 44 wherein the germanium is impregnated into the silica opal template by one of laser ablation of Ge atoms, molecular beam deposition of Ge atoms or infiltration of colloidal germanium, germanium nanoclusters or germane-based polymers using one of either vapor impregnation, solution impregnation and melt impregnation.

55. A method of growing an inverse germanium opal with a complete three dimensional photonic bandgap, comprising:

providing a three dimensional silica opal template including substantially mono-disperse silica spheres having a diameter in a range from about 1.0 to about 2.0 microns;

infiltrating voids in the silica opal template with enough germanium to fill between about 80% to about 100% of said voids; and

etching all the silica out of the template to produce an inverse germanium opal.

56. The method according to claims 55 wherein the silica opal template is infiltrated by chemical vapor deposition using digermane (Ge_2H_6) gas as a precursor.

57. The method according to claims 55 wherein the germanium is selected from the group consisting of single crystal germanium, polycrystalline germanium, nanocrystalline germanium, porous germanium and amorphous germanium.

58. The method according to claims 56 or 57 wherein after infiltrating the silica opal template with germanium the infiltrated template is annealed to assist

diffusion of germanium into the voids in the template to provide substantially uniform spatial distribution of germanium in said voids.

59. The method according to claims 55, 56, 57 or 58 wherein the three dimensional template has dimensions in a range from $2 \times 2 \times 2$ unit cells to $a \times b \times c$ unit cells, wherein $2 < a < 10,000$, $2 < b < 10,000$, $2 < c < 10,000$.

60. The method according to claims 55, 56, 57 or 58 having a planar thin film geometry with dimensions in a range from $1 \times 10 \times 10$ unit cells to $a \times b \times c$ unit cells, wherein $1 < a < 100$, $10 < b$, $c < 100,000$.

61. The method according to claims 35, 36, 37, 38, 39, 40, 41, 42, 43 or 44 wherein said germanium is infiltrated into said three dimensional opal template by infiltration of a germanium-based compound within the voids said opal template, then hydrolyzing said germanium-based compound to form germanium oxide, and then reducing the germanium oxide to germanium in a reducing atmosphere at an effective temperature.

62. The method according to claim 61 wherein said germanium-based compound is a germanium alkoxide.

63. The method according to claim 61 wherein said germanium-based compound is selected from the group consisting of germanium alkoxides, germanium glycolates, germanium halides, alkylgermaniumhalides and alkylgermaniums.

64. The method according to claim 61 wherein said germanium-based

compound is a germanium salt selected from the group consisting of germanium nitrates, germanium acetates, germanium sulfates and germanium oxalates.

65. The method according to claims 61, 62, 63 or 64 wherein said infiltration of said germanium-based compound into said voids followed by hydrolyzing to form germanium oxide is repeated an effective number of times until the germanium is interconnected throughout said template.

66. The method according to claim 62 wherein said germanium alkoxide is tetramethoxyorthogermanate ($\text{Ge}(\text{OCH}_3)_4$).

67. The method according to claim 66 wherein said opal template is infiltrated with said tetramethoxyorthogermanate at room temperature.

68. The method according to claims 61, 62, 63, 64, 65, 66 or 67 wherein said reducing atmosphere includes hydrogen.

69. The method according to claims 65 wherein said germanium oxide is reduced in the presence of hydrogen at a temperature of in a range of 800 to 850 K.

1/10

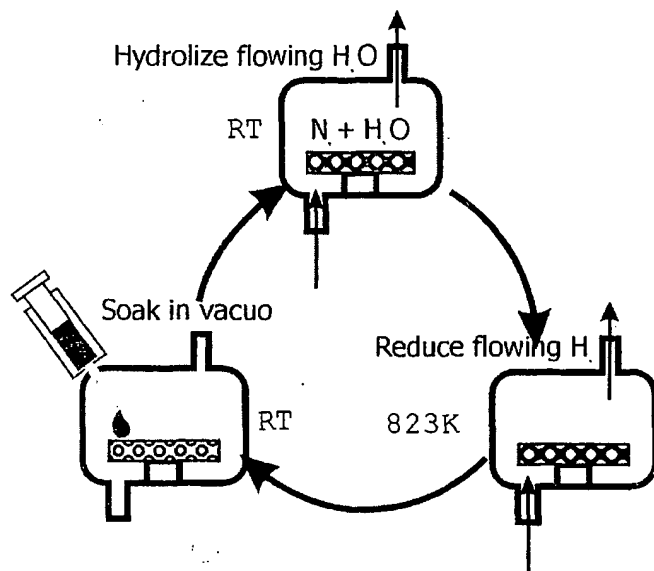


Figure 1

2/10

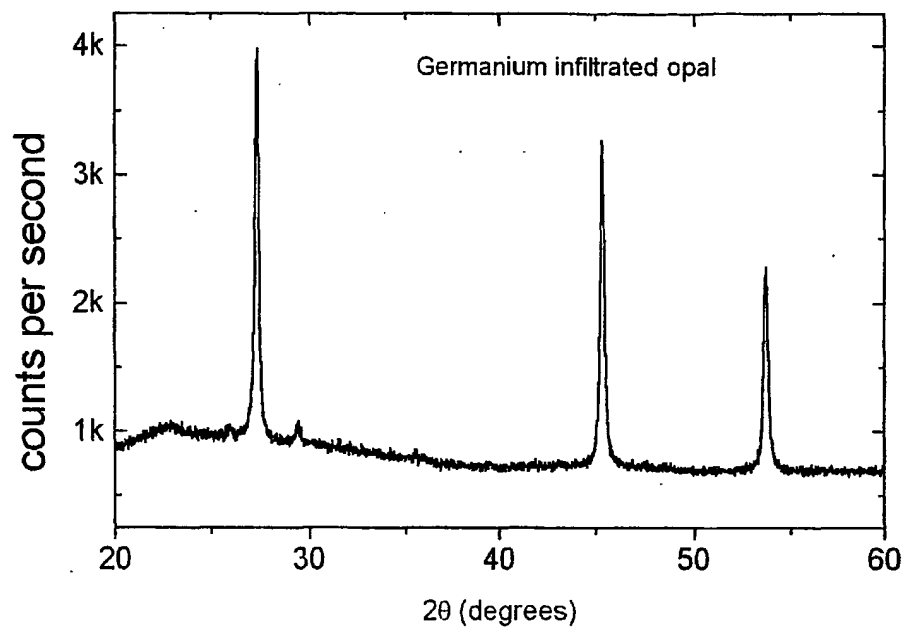


Figure 2

3/10

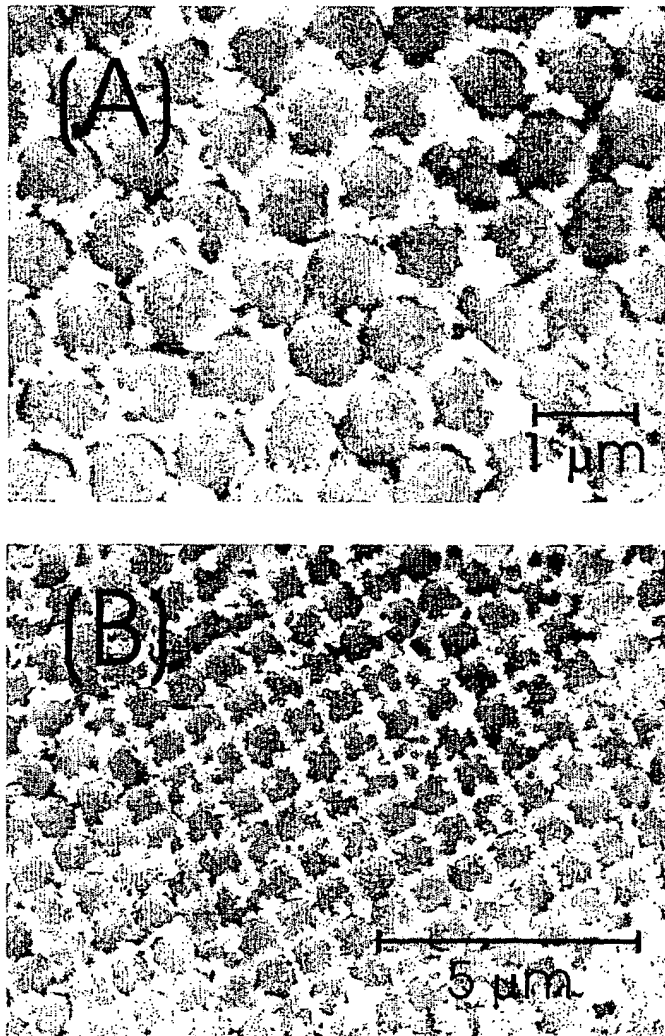


Figure 3

4/10

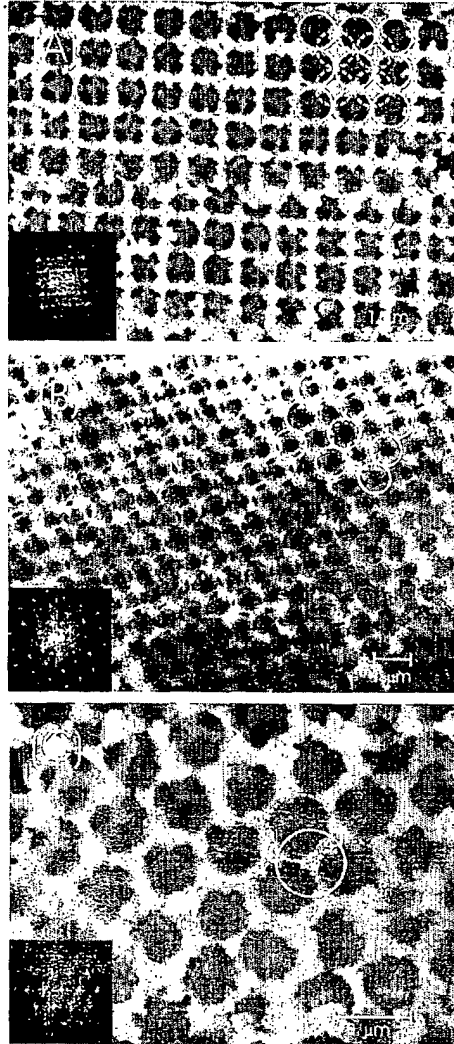


Figure 4

5/10

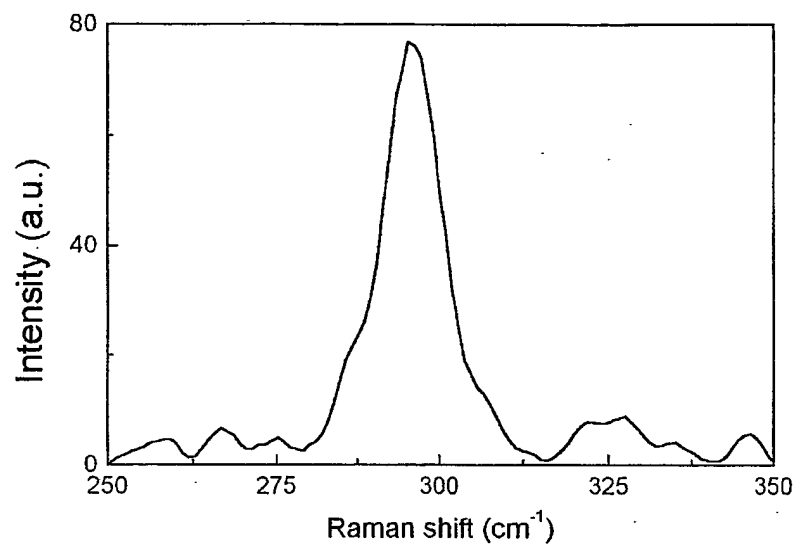


Figure 5

6/10

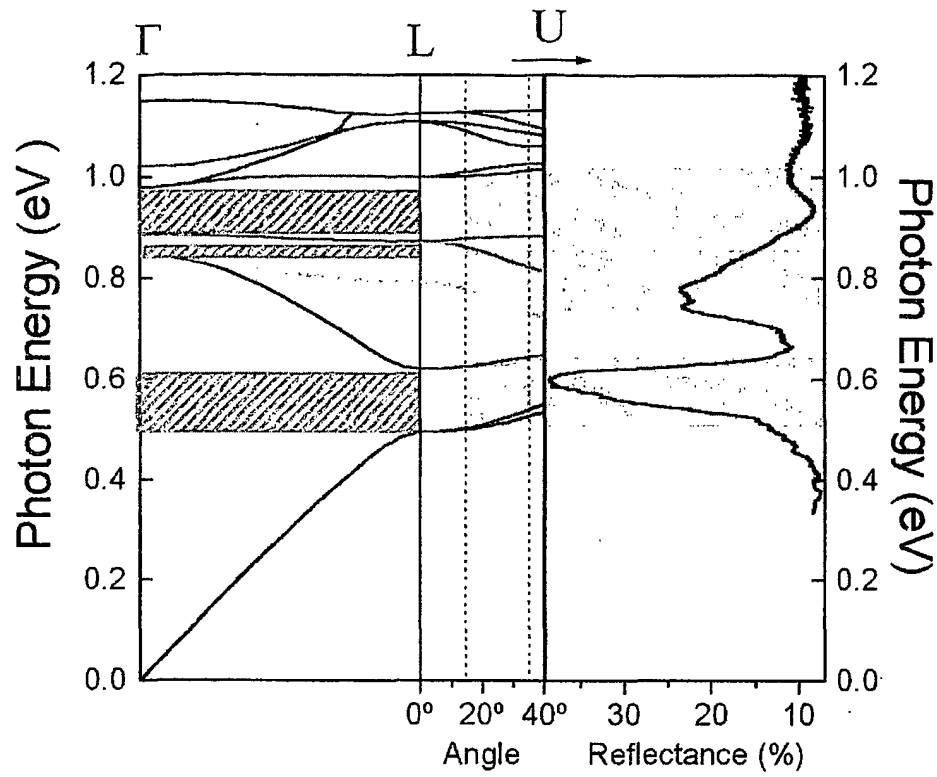


Figure 6

7/10

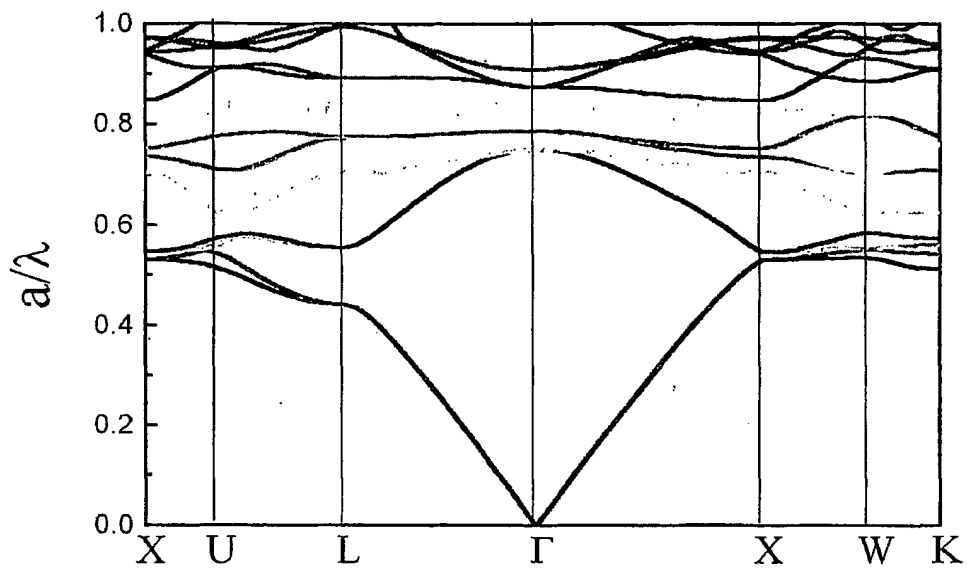


Figure 7

8/10



Figure 8

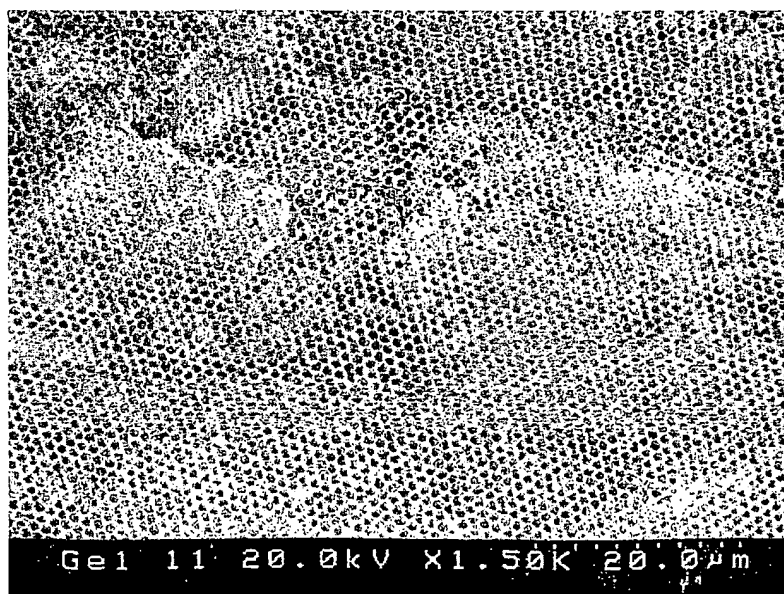


Figure 9

9/10

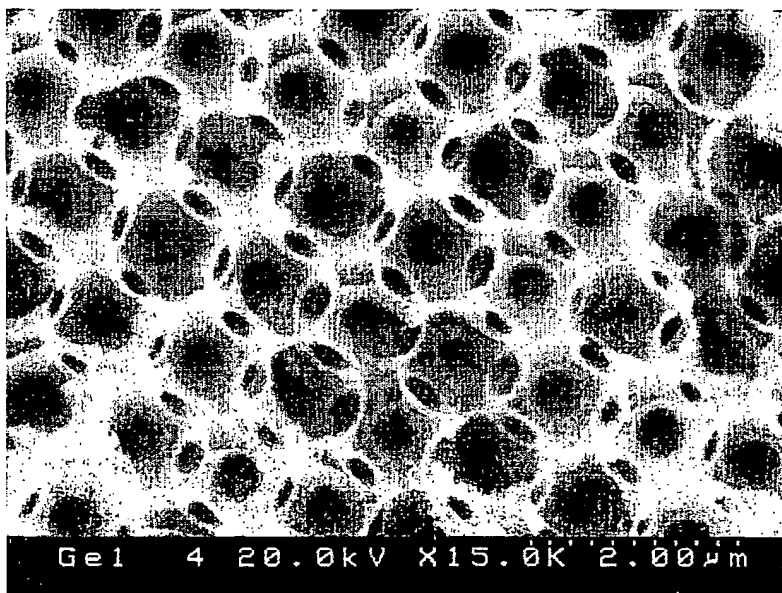


Figure 10

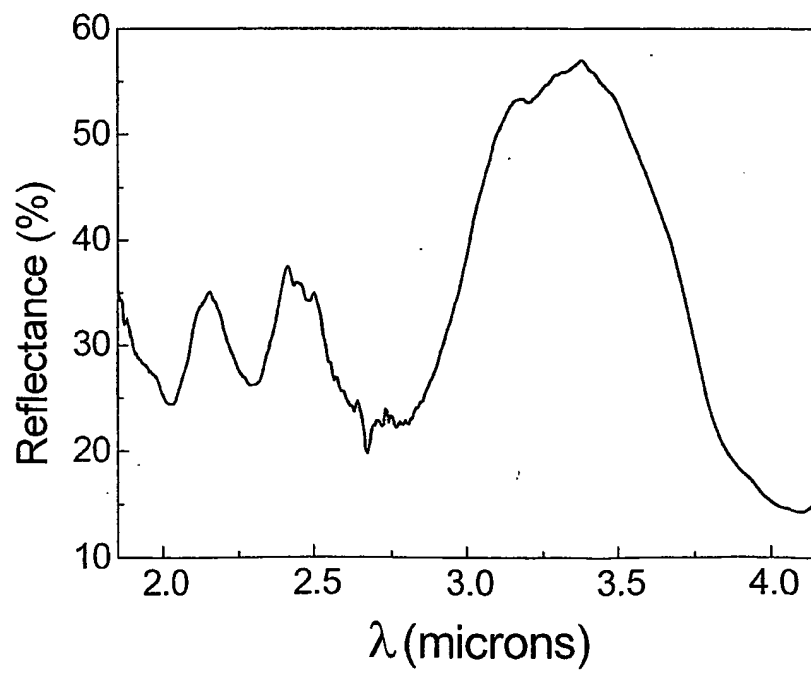


Figure 11

10/10

Ge inverse Opal
12.68% 0.838

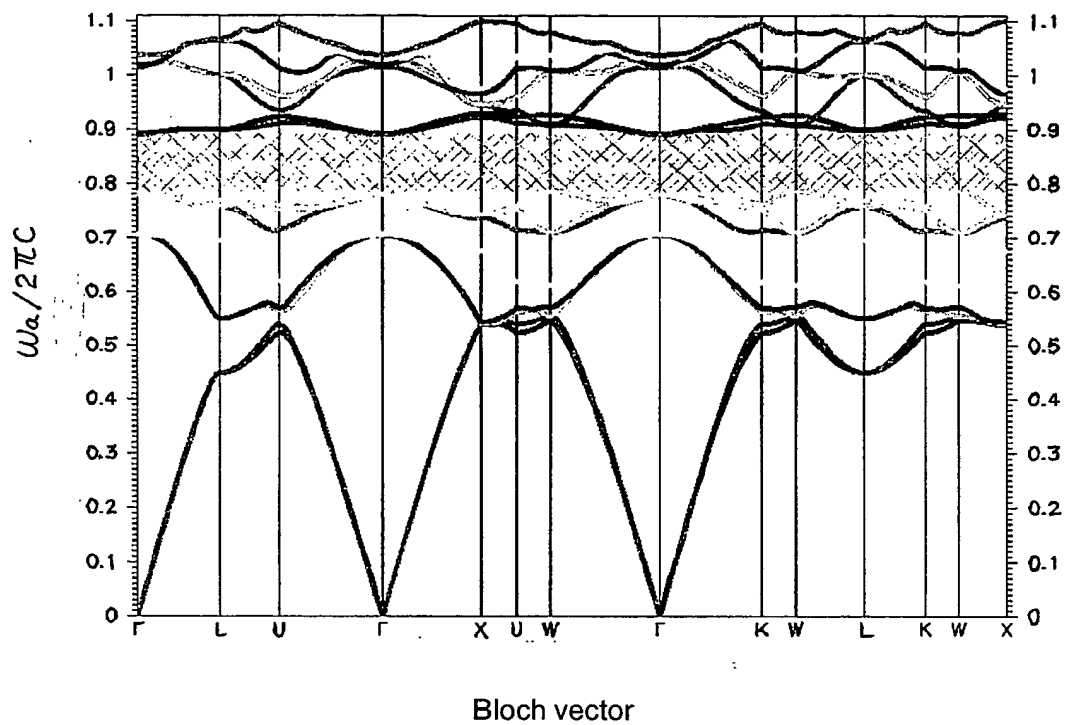


Figure 12

**This Page is Inserted by IFW Indexing and Scanning
Operations and is not part of the Official Record**

BEST AVAILABLE IMAGES

Defective images within this document are accurate representations of the original documents submitted by the applicant.

Defects in the images include but are not limited to the items checked:

- ☐ BLACK BORDERS
- ☐ IMAGE CUT OFF AT TOP, BOTTOM OR SIDES
- ☐ FADED TEXT OR DRAWING
- ☐ BLURRED OR ILLEGIBLE TEXT OR DRAWING
- ☐ SKEWED/SLANTED IMAGES
- ☒ COLOR OR BLACK AND WHITE PHOTOGRAPHS
- ☐ GRAY SCALE DOCUMENTS
- ☐ LINES OR MARKS ON ORIGINAL DOCUMENT
- ☐ REFERENCE(S) OR EXHIBIT(S) SUBMITTED ARE POOR QUALITY
- ☐ OTHER: _____

IMAGES ARE BEST AVAILABLE COPY.

As rescanning these documents will not correct the image problems checked, please do not report these problems to the IFW Image Problem Mailbox.